PHYSICAL REVIEW B, VOLUME 63, 014408

Inhomogeneous structure and magnetic properties of granular $Co_{10}Cu_{90}$ alloys

P. Panissod,[1] M. Malinowska,[1,2] E. Jedryka,[1,2] M. Wojcik,[2] S. Nadolski,[2] M. Knobel,[3] and J. E. Schmidt[4]
[1]*Institut de Physique et Chimie des Matériaux de Strasbourg, 67 037 Strasbourg, France*
[2]*Institute of Physics, Polish Academy of Sciences, 02 688 Warszawa, Poland*
[3]*Instituto de Física Gleb Wataghin, Universidade Estadual de Campinas 13083-970, Campinas, SP, Brazil*
[4]*Instituto de Física, Universidade Federal do Rio Grande do Sul, 91501-970, Porto Alegre, RS, Brazil*
(Received 2 November 1999; revised manuscript received 12 May 2000; published 11 December 2000)

Granular $Co_{10}Cu_{90}$ alloys displaying giant magnetoresistance have been obtained by melt spinning followed by an appropriate heat treatment in the range 0–700 °C. Their structural and magnetic properties have been studied on a microscopic scale using ^{59}Co NMR technique and thermoremanent magnetization measurements. The study reveals that in the as-quenched samples Co is involved in two main structural components: small, irregular, strained Co particles (60% of the entire Co population) and a composition modulated CoCu alloy. A high modulation amplitude of the concentration profile in the alloy subdivides the latter in two parts with distinctly different properties. One part consists of ferromagnetic alloy (average Cu concentration of about 20%) with a blocking temperature of about 35 K (involving 6% of the entire Co population in a sample). The other part, containing the remaining 34% of the entire Co population, is a paramagnetic alloy with a blocking temperature below 4.2 K. The ferromagnetic alloy is magnetically soft—its transverse susceptibility is lower by a factor of 7 than the transverse susceptibility of the quenched-in Co particles. The latter population has a blocking temperature of about 150–200 K. During the heat treatment, each of the two main structural components undergoes respective decomposition processes: both of them display two temperature regimes. One process consists in dissolving the quenched-in Co particles after annealing at around 400 °C, followed at higher temperatures by a nucleation and growth of the more regular in shape Co particles. The other process resembles a spinodal decomposition of the quenched-in CoCu alloy, resulting in sharpening of the concentration profile and eventually leading to Co cluster formation in samples annealed above 450 °C. Both processes end at about $T_{an}=700$ °C, in formation of large, pure Co clusters that are ferromagnetic at least up to 400 K.

DOI: 10.1103/PhysRevB.63.014408 PACS number(s): 75.50.Kj, 83.80.Fg, 75.20.En, 76.60.Lz

I. INTRODUCTION

Granular magnetic systems have been deeply studied in the last 50 years, after the pioneering work by Stoner and Wohlfarth.[1] Besides the obvious technological importance in magnetic recording, these systems provide an unique setting to investigate several interesting properties, such as superparamagnetism, kinetics of crystal nucleation and growth, and spin-glass-like behavior (see, e.g. Ref. 2). In the last few years, the interest in granular systems has been reinforced by the discovery of the so-called giant magnetoresistance effect (GMR), when the granular structure is composed of two metallic elements (e.g., Fe-Ag, Cu-Co).[3,4] More recently, other systems such as metal-insulator nanocomposites have also shown interesting magnetotransport properties, such as tunnel magnetoresistance and giant Hall effect.[5] The materials nanostructure can be suitably controlled by means of specific thermal treatments,[6] and it is found that both the magnetic properties and magnetoresistance strongly depend on the inherent nanoscopic structure, i.e., the distribution of grain sizes, the mean intergrain distance, the shape of the crystallites and the magnetic/nonmagnetic interfaces.

In the particular case of Cu-Co heterogeneous alloys, produced either by melt spinning or sputtering, the hysteresis loops display a superparamagneticlike behavior at room temperature, but with a small, but well-defined, coercive field and remanence.[7,8] The origin of such hysteresis (and its thermal dependence) was yet not fully clarified, being attributed either to interparticle interactions,[9] and/or the presence of a small quantity of big, blocked grains at high temperatures.[10] The main problem is that conventional structural analysis methods are hardly applicable here, owing to the low x-ray contrast between Co and Cu as well as to the high lattice coherency and small lattice mismatch (<2%). Nonetheless, some structural information on the melt spun $Cu_{90}Co_{10}$ alloys has been obtained from atom probe/field ion microscopy (AP/FIM) and transmission electron microscopy (TEM) studies.[11–14] In addition, some aspects of the nature of the cobalt-copper mixing and its evolution with annealing treatment could be inferred from the analysis of bulk magnetization data.[15,16] However, information resulting from these structural studies is not consistent throughout the literature. While magnetization measurements show the presence of a fraction of ferromagnetic Co clusters in the as-quenched state, some FIM and TEM studies failed to reveal directly such clusters. On the other hand, an autocorrelation analysis of the FIM (Ref. 13) did show the existence of Co-rich clusters. Actually, the density of quenched-in Co clusters may depend significantly on the preparation conditions and in particular on the grain size, since Co clusters nucleate preferentially at grain boundaries.[11] Co concentration of 10 at. % seems to be an upper limit to prepare homogeneous alloys by rapid quenching. For larger Co contents the microstructure is determined by a competition between polymorphic solidification from the melt and spinodal decomposition of the supersaturated solid solution.[11] After an annealing treatment at around 440 °C (which yields the largest GMR values) both research groups[11,13] agree on the presence of Co granules.

However, FIM and TEM studies show that besides the Co granules located at grain boundaries, a fraction of cobalt atoms is still dispersed in the copper grains where a spinodal-like decomposition takes place with a large concentration modulation. No statistical investigation was undertaken to quantify the amount of Co in these two phases, though.[12] In another AP/FIM study the authors have undertaken a statistical study of the Co granule density and size distribution in a $Cu_{88}Co_{12}$ sample.[13] From their results the volume fraction of the granules can be estimated to be between 4 and 6%, which represents only 40–50 % of the Co atoms. In any case, samples with optimum GMR performance were reported to contain segregated Co, both as spheroidal clusters and as atomically dispersed atoms in a concentration modulated alloy.

In this work we have performed a detailed structural and magnetic study of granular samples obtained by annealing a melt-spun $Co_{10}Cu_{90}$ ribbon. Exactly the same sample was previously investigated by conventional magnetometery and magnetoresistance,[15,17] leading to magnetoresistance ratios up to 15% at room temperature for samples annealed for 1 h at 450 °C. In the present work we analyze the behavior of the thermoremanent magnetization (TRM), which provides relevant information about the distribution of blocking temperatures within the samples,[18] clearly revealing the existence of three different phases. Furthermore, NMR was used to obtain detailed microscopic information on the structure and local magnetic properties, providing interesting insights into the structural and magnetic characterization of granular magnetic materials. In a previous paper we have reported the use of ^{59}Co NMR to study such a correlation in the as-quenched melt-spun $Co_{10}Cu_{90}$ ribbon.[19] The yield of NMR experiments is twofold: On one hand the NMR spectrum reflects the distribution of hyperfine fields in the sample and thus gives an information about the structure, defects, strains, and, in particular, on the chemical coordination distributions in the various phases present in a composite sample. On the other hand the rf field required to obtain the maximum NMR signal probes the magnetic stiffness (the transverse magnetic susceptibility) of the electronic moments around the nucleus site, thus providing an information comparable to that given by ferromagnetic resonance (FMR) measurements.

Therefore, combining both aspects of NMR, together with the TRM results, it was possible to correlate the inhomogeneous magnetic properties of a composite sample with its different structural components. As a result, a clear picture of this complex nanostructured material is obtained, which can help to elucidate many open questions related to its magnetic and magnetotransport properties.

II. EXPERIMENTAL RESULTS AND ANALYSIS

A. NMR

A rapidly quenched $Co_{10}Cu_{90}$ ribbon was prepared by melt spinning in a controlled He atmosphere on a CuZr drum. Different pieces cut from that ribbon were subsequently submitted to furnace annealing for 1 h under argon atmosphere at temperatures in the range 250–700 °C.[16] ^{59}Co NMR experiments have been carried out at 4.2 K using an automated, phase sensitive spin-echo spectrometer.[20] The spectra have been taken every 1 MHz in the frequency range 50–240 MHz at several values of the rf field amplitude, covering a range of field values within more than one order of magnitude. Figure 1 presents raw experimental spectra recorded from the studied series of samples at two exemplary values of rf field amplitude: a low [Fig. 1(a)] and a high [Fig. 1(b)] rf field amplitude. All the spectra in Fig. 1 have been normalized in order to bring out the differences in the intensity distribution. The most remarkable feature is that a low rf field favors the low-frequency part of the spectrum (resonance condition for Co having a significant number of Cu nearest neighbors), while a high rf field provides the optimum condition for exciting the NMR signal in the frequency range close to pure fcc Co (217 MHz in the bulk[21]).

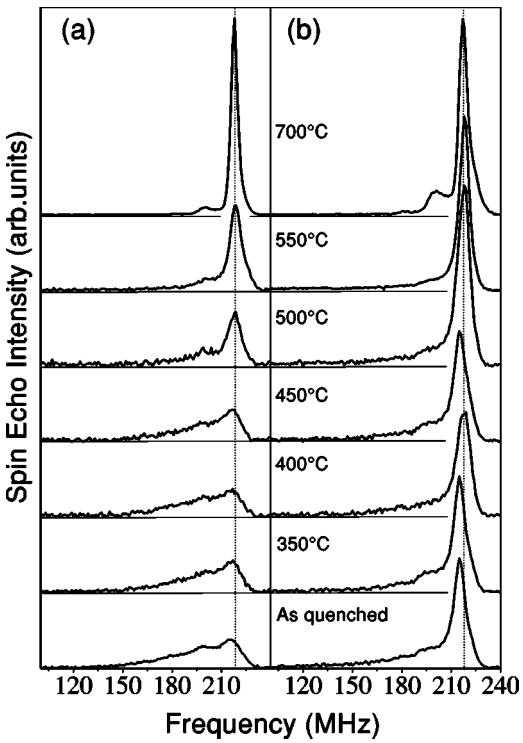

FIG. 1. ^{59}Co NMR spectra from the $Co_{10}Cu_{90}$ melt spun ribbons heat treated at different temperatures. The spectra were recorded at 4.2 K for the low (a) and high (b) rf power, respectively. The vertical dotted lines describe the frequency position of fcc Co.

The shape of raw NMR spectra does not change significantly upon annealing up to 400 °C, neither for the low nor for the high rf field amplitude. For samples annealed at 500 °C and higher, the spectra in Fig. 1(a) become progressively single peaked, i.e., cobalt is less and less mixed with copper, while the Co peak in Fig. 1(b) recovers rapidly a high intensity at 215 MHz, then shifts progressively to higher frequencies. For samples annealed at temperatures higher than 550 °C, the spectrum shape is practically independent of the rf power. The Co peak has a maximum at 217 MHz, which is the classical NMR frequency of fcc Co. On the low-frequency side of the Co peak the NMR spectrum still displays a weak satellite structure, revealing the presence of a small amount of copper embedded in a single cobalt phase.

A more rigorous analysis can be performed based on the theory of NMR signal.[22] It predicts that the spin-echo intensity at each frequency can be expressed as a function of the rf field amplitude H_1 in the following way:

$$S(H_1,\omega)=\eta I_0(\omega)\omega^2 \exp[-\log_{10}{}^2(H_1/H_{1\mathrm{opt}})/2\sigma^2], \quad (1)$$

where $I_0(\omega)$ is the ''true'' signal intensity—proportional to the number of nuclei—$H_{1\mathrm{opt}}$ is the rf field value for which the signal is maximum, η is the NMR enhancement factor and σ is the width of the Gaussian distribution in $\log_{10}(H_1)$. Experimentally σ is found in the range 0.7–1.2 for typical ferromagnetic samples. It can easily be shown[19] that $H_{1\mathrm{opt}}$ is related to sample's restoring field H_r in the following way:

$$H_r=(2\tau/\pi)\gamma H_{\mathrm{hf}}\cdot H_{1\mathrm{opt}}=(2\omega\tau/\pi)H_{1\mathrm{opt}}=\beta H_{1\mathrm{opt}}, \quad (2)$$

where γ is the nuclear gyromagnetic ratio, H_{hf} is the hyperfine field, and τ is the pulse length used in the experiment. The value of β being known, this simple relation allows one to discuss NMR results in terms of restoring field, a material property that is easily understood, rather than in terms of the optimum excitation field, a notion for the specialists. H_r is the restoring field reflecting the energy dependence of the electronic moments upon small orientation changes. For example, it takes the value of anisotropy field for a uniaxial, single domain particle. In other words $1/H_r$ is proportional to the local transverse electronic susceptibility. In the following, we shall always express H_1 in units of H_r (i.e., we shall use βH_1 instead of H_1).

From Eq. (1) it follows that the signal intensity has a gaussian dependence upon $\log_{10}(H_1)$. To reconstruct this curve, we carry out the experiment routinely at several values of the rf power and, for each frequency, we fit the Gaussian evolution of the signal intensity using a least-square procedure. If a material consists of several phases, more than one Gaussian is needed to describe the signal intensity as a function of the excitation field. In Ref. 19 we have shown that this was the case of the as-quenched ribbon, which was the starting material for preparing the present samples: at each frequency two Gaussian distributions were fitted. Present experiment shows that the studied samples remain multiphase materials up to the annealing temperature of 700 °C. This is exemplified in Fig. 2, where we plot the NMR signal intensity recorded from the sample that has been annealed at 350 °C as a function of excitation field strength for two exemplary frequencies: 200 MHz (full circles) and 215 MHz (full squares). At both frequencies two Gaussian distributions had to be used: one centered at about $H_{r1}\sim 1880$ Oe and the other one at $H_{r2}\sim 14\,000$ Oe. At 200 MHz the two components have comparable amplitudes, while at 215 MHz the harder component is clearly dominant. Such fit has been computed for every experimental frequency point, which allowed to separate the spectra arising from each of the two phases present in every sample and to determine their average restoring field. The final NMR spectra computed in such way from the experimental ones are presented in Fig. 3(a) (soft magnetic phase) and Fig. 3(b) (hard magnetic component). A possibility that the two H_r values correspond to domain wall and domain excitation regimes, respectively, is excluded considering the obviously different hyperfine field distributions in Figs. 3(a) and 3(b).

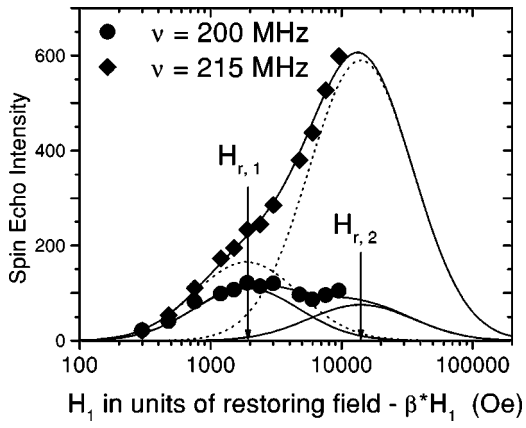

FIG. 2. Spin-echo intensity at 200 MHz (full circles) and 215 MHz (full squares) as a function of rf field strength expressed in the units of βh_1. The data were recorded in the $Co_{10}Cu_{90}$ melt spun alloy annealed at 350 °C and represent similar properties observed in all samples up to 450 °C annealing temperature. Dotted lines: the two Gaussians fitted to the spectrum at 215 MHz; full lines: fits to the spectrum at 200 MHz.

The bottom panels in these figures correspond to the two phases in the as-quenched samples, and their evolution with the annealing temperature is presented in the panels above them. The great majority (90%) of ferromagnetic Co atoms in the as-quenched sample are found in a hard phase, represented in Fig. 3(b). The dominating feature in this NMR spectrum is a strong Co peak at 215 MHz, revealing the presence of fcc Co. The high restoring field of the hard phase

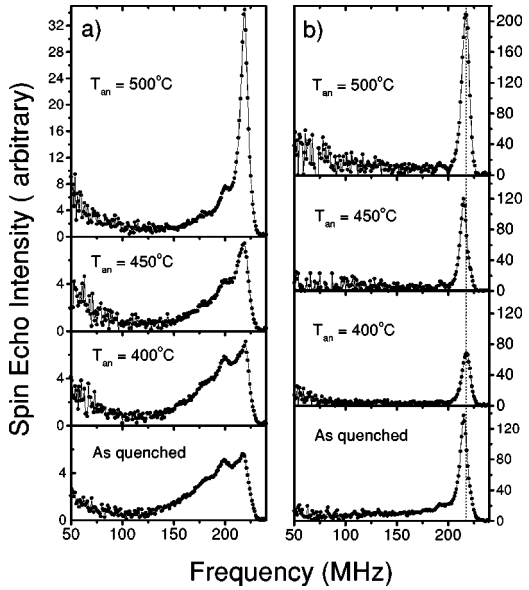

FIG. 3. Magnetically soft (a) and hard (b) components of the NMR spectrum recorded at 4.2 K in $Co_{10}Cu_{90}$ melt spun ribbons annealed at different temperatures. The decomposition has been performed using the procedure described in text. The vertical dotted line in the (b) panels describes the frequency position of fcc Co.

suggests that these Co agglomerates are single domain particles. The NMR frequency in bulk fcc Co is 217 MHz; the slightly lower frequency observed here results from the expansive strains in these small agglomerates[23] which decrease the hyperfine field (and thus the NMR frequency). The low-frequency component in the NMR spectrum corresponding to the hard phase is strikingly similar to the spectrum observed in Co/Cu multilayers with rough interfaces and limited interdiffusion.[24] The interfacial intensity amounts to about 50% of the hard phase spectral intensity indicating that these Co agglomerates have a large surface-to-volume ratio, which can be understood if they are flat (typically four atomic layers thick) or needlelike (with a typical diameter of five atomic distances).

The remaining 10% of ferromagnetic Co atoms in the as-quenched state are found in the magnetically soft phase, represented in Fig. 3(a). This NMR spectrum is typical of a CoCu alloy—it shows a characteristic structure of satellites separated by about 16 MHz on the low-frequency side of the Co peak. These satellites correspond to Co first coordination shells with one, two, etc., Cu neighbors as previously reported for random CoCu alloys.[21] However, the spectrum shape for the soft phase is not the one expected for a homogenous alloy since it deviates from the binomial distribution of impurity atoms, indicating the existence of large concentration fluctuations. At least two components, with respective Cu content of 5 and 24 % are needed to describe the intensity distribution in the spectrum, as shown in Fig. 4. Actually, in order to fit the low-frequency upturn in spectra, a third component (with Cu content of about 83%) would be necessary. The soft magnetic phase represents areas of quenched-in Co rich alloy where atomically dispersed Co atoms are coupled enough to behave ferromagnetically at 4.2 K.

For samples annealed at low temperatures, up to 350 °C, no significant evolution of either of the two phases is observed with respect to the as-quenched sample. In the soft magnetic phase the distribution of atomically dispersed Co atoms within the copper matrix starts changing for annealing temperatures above 400 °C. The concentration profile of these particles becomes sharper and sharper as a result of annealing. Figure 4 presents the fits to the NMR spectra from the soft component for the selected samples. For $T_{an} = 450$ °C the Co concentration increases in both alloy components (Cu content drops from 24 to 18 % and from 5 to 2.9 %, respectively). The enrichment in Co eventually leads to a new component in the fits: a pure Co line must be added for the sample annealed at 500 °C. This means that a core of pure Co starts to develop inside the alloyed particles and the spectrum of the soft phase starts to resemble that of the hard phase.

The hard magnetic phase [Fig. 3(b)] undergoes a different kind of evolution. At 400 °C rapid changes start to take place: the intensity of that signal decreases abruptly while the soft magnetic phase remains practically the same as in the as-quenched sample. In the hard phase, the peak at 215 MHz together with its characteristic low-frequency profile disappears and only a low intensity peak at the usual Co frequency of 217 MHz remains. In fact, a trace of that peak is already present in the spectrum recorded from the as-quenched sample in form of a shoulder at 217 MHz. For annealing temperatures higher than 450 °C the intensity of the Co peak at 215 MHz increases again, but the low-frequency profile observed in the as-quenched sample does not reappear. Clearly, at higher annealing temperatures Co clusters take a different shape or a different interface profile than the one observed in the as-quenched sample. The low interfacial intensity shows that the Co precipitates formed as a result of annealing are more regular in shape, with a minimum amount of surface area and virtually no interdiffusion at the interface. As the annealing temperature increases, the newly developed peak shifts progressively towards the usual fcc Co frequency.

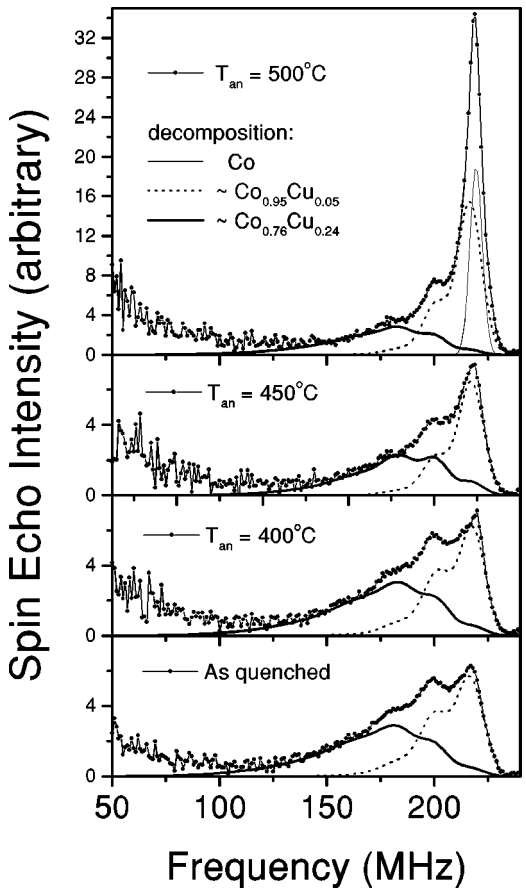

FIG. 4. Decomposition of the magnetically soft part of $Co_{10}Cu_{90}$ melt spun ribbons. A combination of two CoCu random alloys describes the concentration modulated composition of samples annealed up to 450 °C. The alloy compositions quoted in the figure apply to the as-quenched sample—their evolution with annealing temperature is described in the text. For sample annealed at 500 °C a new line corresponding to pure Co component has to be added in the fit.

Above 550 °C the separation of the two phases was not possible, because the shape of their NMR spectra and their restoring fields become very similar. Eventually the sample becomes a single, homogeneous magnetic phase essentially consisting of fcc Co clusters. The analysis of the spectral shape for $T_{an} = 700$ °C shows that the copper content in the cobalt clusters is only 1% on average although copper atoms are not randomly distributed in all clusters. The best fit to the

TABLE I. Atomic fractions of cobalt in the three different phases as deduced from the NMR analysis of the $Cu_{90}Co_{10}$ melt spun samples, as-quenched and after 1 h annealing at various temperatures (T_{ar}). Results are in % of the intensity observed in the single phased sample annealed at 700 °C for which one assumes that all Co nuclei are observed.

T_{ar} (°C)	Paramagnetic[b]	Soft alloyed particles	Hard pure Co particles
As-quenched	34	6	60
350	38	7	55
400	70	7	24
450	64	5	31
500	22	12	66
550			
600			
700[a]	0		100

[a]Single ferromagnetic population.

[b]Since this population is only partly and inaccurately observed, the value shown is the complement to 100 of the sum of the two other fractions.

spectral shape is obtained taking $Cu_{0.04}Co_{0.96}$ alloy to account for $\frac{1}{4}$ of the total spectrum intensity and pure Co for the remaining $\frac{3}{4}$. This is certainly reminiscent of the initial inhomogeneity of the cobalt dispersion in the as-quenched sample.

The quantitative results in terms of fractions of the different phases are summarized in Table I, assuming that 100% of the cobalt is observed in the sample annealed at 700 °C.

In parallel to changes in the spectrum shape and intensity, a variation of the magnetic stiffness of the two respective phases takes place upon annealing, as shown in Fig. 5. Softening of the hard magnetic phase could be associated with

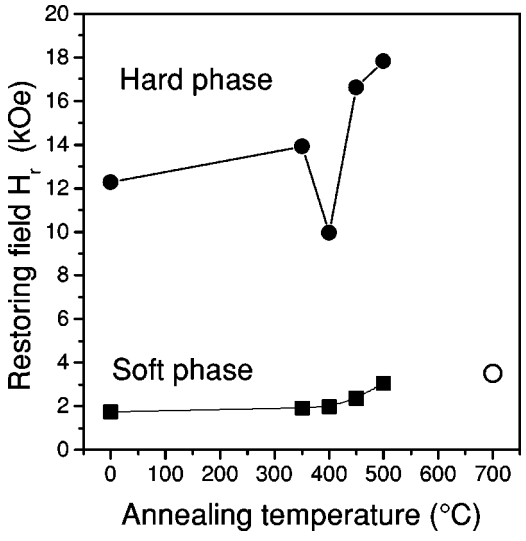

FIG. 5. The NMR restoring field in the soft (squares) and hard (circles) magnetic phases of $Co_{10}Cu_{90}$ melt spun ribbons as a function of annealing temperature. A drop at 400 °C of the restoring field in the hard phase corresponds to a transition between the irregular and spherical Co particles.

disappearance of the quenched-in Co agglomerates, in agreement with the previous suggestion that only the largest, unstrained, and most regular Co clusters remain as a result of annealing at around 400 °C. The subsequent growth of new small Co grains causes again a stiffness increase of the hard phase, even above the value found in the as-quenched sample. The generally high restoring field of this phase (around 12.8 kOe in the as-quenched sample) is very probably related to anisotropy contribution resulting from magnetoelastic interactions. Such conclusion is supported by the strong correlation between the value of the restoring field and the frequency downshift due to the lattice strain of Co particles. Indeed, the Co particles formed at the temperatures $T<350$ °C and $450<T<500$ °C are characterized by frequency of 215 MHz and a high value of the restoring field. The latter decreases for large, unstrained Co particles, formed at temperatures around 400 °C, characterized by the usual (for fcc Co) frequency of 217 MHz. The smaller value of the restoring field observed for the alloyed component (about 1.8 kOe in the as-quenched sample) can be understood as resulting from self-averaging by the exchange interaction of the random anisotropy due to the CoCu admixture. The magnetic stiffness of this soft phase starts to increase slightly in the sample annealed at 500 °C—this is the point where the pure Co cores start to be visible in the NMR spectra.

After annealing at 700 °C the restoring field in the ferromagnetic phase, now homogeneous, is about 3.6 kOe (the open circle in Fig. 5), slightly larger than in the alloyed soft phase and significantly lower than in the hard phase.

In the sample that was annealed at 700 °C the total amount of Co (estimated from the intensity of the NMR signal) is about 30% higher than the amount of Co contained in both phases (soft and hard) in the as-quenched sample. This means that in the as-quenched state at least 30% of the Co atoms are located in a CoCu alloy which is nonmagnetic at 4.2 K and thus are not detected by zero-field NMR. In this way the NMR results indicate implicitly the presence of the third, not magnetic phase—this phase was further confirmed by the thermoremanence studies, described in the following section.

B. Thermoremanent magnetization

In order to get additional information on the magnetic phases present in the samples, we have carried out thermoremanent magnetization (TRM) measurements using a superconducting quantum interference device (SQUID) magnetometer. The experimental procedure consisted in cooling the sample down to 4.2 K in a field of 10 kOe, followed by magnetization measurements at increasing temperatures. At each temperature point the sample was magnetized in a field of 10 kOe for 1 min—after that time the field was switched off and the sample was allowed to relax for 1 min. The remanent magnetization measured after this field cycle is a measure of the magnetic moment of all clusters that are still blocked at a given temperature for a time scale of 60 s. It reflects the probability to find Co in clusters with a blocking

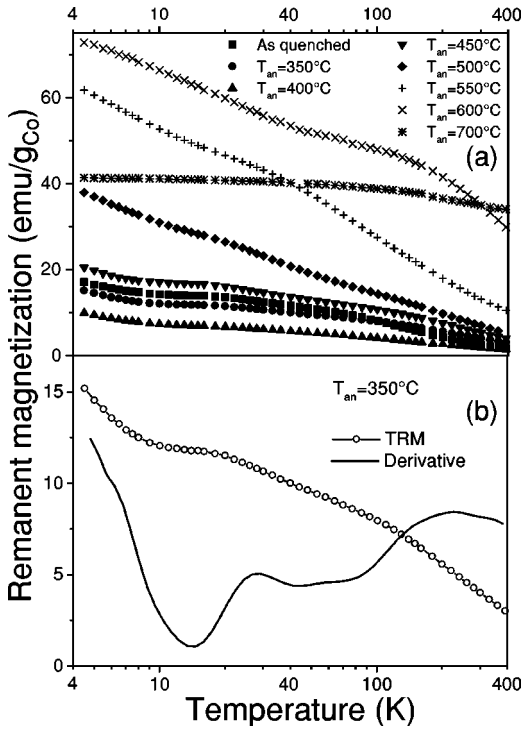

FIG. 6. (a) Thermoremanent magnetization (TRM), measured by SQUID magnetometer in $Co_{10}Cu_{90}$ melt spun ribbons: as-quenched and subject to annealing at different temperatures. (b) TRM curve measured in a sample annealed at 350 °C and its temperature derivative.

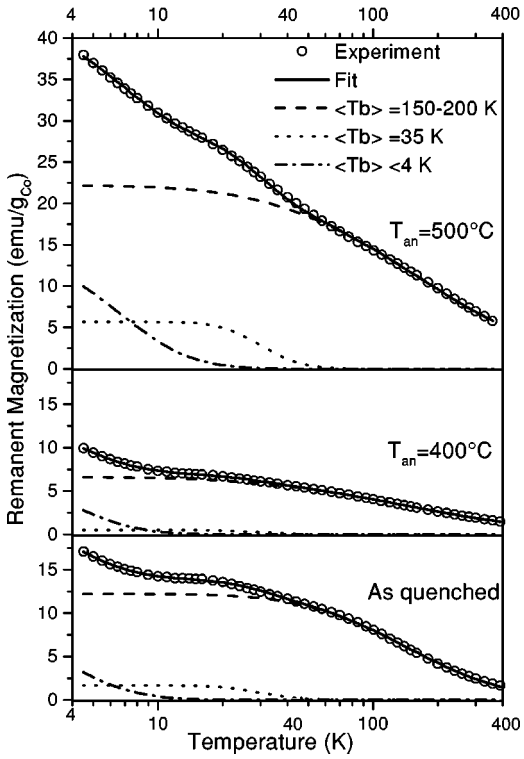

FIG. 7. Fitting the experimental TRM curves with three $\{1-erf[\ln(T)]\}$ partition functions exemplified for three samples of $Co_{10}Cu_{90}$ melt spun ribbons. For details see text. Quantitative results of this decomposition are presented in Table I.

temperature (T_b) higher than the measurement temperature T, i.e., the complementary partition function of the blocking temperatures.[18]

Broad distributions of sizes (or blocking temperatures) are usually assumed to have a lognormal character, therefore we present our data in a ln(T) scale. A single lognormal distribution of blocking temperatures would appear in such a plot as a sigmoidal curve, $\{1-erf[\ln(T)]\}$. Our experimental plots presented in Fig. 6(a) are more complex than that. With the exception for the sample annealed at 700 °C, most TRM curves reveal three smeared steps at around 150–300 K, 30–50 K, and below 10 K. To bring out the details of the TRM variation, Fig. 6(b) presents an example of the temperature derivative of the TRM curve, which reflects the distribution of blocking temperatures. This derivative shows clearly three broad, bell-shaped distributions. One is a large population of particles the blocking temperature of which is centered around $T_b = 200$ K and extends considerably above room temperature. The other is a smaller population of particles with blocking temperatures in the 20–70-K range. The third distribution, the maximum of which is not reached at 4.2 K, corresponds to a large population of particles with blocking temperatures below 10 K—practically a paramagnetic phase.

The evolution of the TRM curves upon annealing initially shows a decrease of the thermoremanent magnetization at all measured temperatures. For samples annealed above $T_{an} = 400$ °C a rapid increase is observed, particularly at low temperatures. The remanent magnetization even goes through a maximum at low temperature for the sample annealed at 600 °C. Actually the changes observed above $T_{an} = 500$ °C indicate not only an increase of the remanent magnetization but also a shift of the whole curve towards higher temperatures, which shows the increase of the volume of all the particles. For $T_{an} = 700$ °C the sample behaves like a homogeneous ferromagnet: all particles are blocked at least up to room temperature. The lower remanent magnetization at low temperatures with respect to the samples that were annealed at 550–600 °C can be understood as due to the development of a domain structure in the largest clusters. In addition, a small part of the cobalt could be dissolved back in the copper matrix as indicated by a slight decrease of the saturation magnetization otherwise very close to that expected from all Co atoms in the sample.[15]

At the same time the effects of interaction between the particles are not excluded in samples obtained by annealing at any temperature. These interactions may be the source of additional reduction of remanent magnetization. As an example of a theoretical approach to this problem one can refer to Monte Carlo simulations of the remanence and coercive field for uniaxial particles interacting through dipole interaction only (in an insulating matrix).[25] One can notice that the calculated remanence is always lower than 0.5 (uniaxial case) and significantly lower if the interaction is large with respect to the anisotropy. One can expect that in a metallic matrix the indirect exchange coupling that can be antiferromagnetic between some (possibly many) of the particles does contribute strongly to the reduction. It is also possible

TABLE II. Remanent magnetization of the three Co populations as deduced from fits to the thermoremanent magnetization measurements of $Cu_{90}Co_{10}$ melt spun samples, as-quenched and after 1 h annealing at various temperatures (T_{an}). Results are in emu/g_{Co} to be compared to that expected for single domain, noninteracting, Co particles: 80 emu/g_{Co} (160×0.5 for uniaxial anisotropy) or 140 emu/g_{Co} (160×0.886 for cubic anisotropy).

T_{an} (°C)	$T_b<10$ K[c]	$\langle T_b\rangle=35$ K	$\langle T_b\rangle=150-200$ K
As made	7.9	1.9	12.0
350	8.9	1.7	10.0
400	6.3	0.5	6.7
450	9.2	3.3	13.4
500	12.1	5.9	22.2
550[a]	14.6	2.5	48.0
600[a]	13.6	8.0	52.0
700[b]			40.5

[a]For $T_{an}=550-600$ °C the average blocking temperatures of the three populations were constrained in the fit to those found for annealing temperatures below 550 °C (4, 35, and 150 K); slightly better fits are obtained using larger T_b's.

[b]Single ferromagnetic population: $\langle T_b\rangle$ larger than 400 K.

[c]Underestimate: part of the Co atoms are still paramagnetic below 4.2 K.

that because of the interactions, either ferro- or antiferromagnetic, collective domains and domain walls can develop across the sample.

Figure 7 presents exemplary fits to the experimental data in three of the samples, using *erf* partition functions in ln(T) scale. In order to fit the experimental data properly, three *erf*'s were necessary, in agreement with the consideration presented above. The Co remanent magnetization components corresponding to these fits are given in Table II and shown later in Fig. 8 together with the quantitative NMR results. The value for the population with the lowest average blocking temperature is underestimated since the plateau of their partition function is not reached at the lowest measurement temperature.

If the various populations observed in the thermoremanent magnetization measurements did not differ in their anisotropy constant K, their average blocking temperature, $T_b=\alpha KV/k_B$, would be a measure of the average particle volume V. However, NMR data indicate that the sample contains several magnetic phases, with distinctly different magnetic stiffness. This implies different magnetic anisotropy, therefore no conclusion can be drawn immediately about particle sizes. On the other hand, if the particles differed mostly by their anisotropy, the different populations evidenced by both techniques could be directly compared. Such comparison and the nature of the particular populations will be discussed in Sec. III in the context of information resulting from the NMR analysis.

At this stage let us merely remark that, in terms of intensity, the overall evolution of the remanent magnetization with increasing annealing temperature parallels closely that of the NMR signal. At 4.2 K it decreases by a factor of 2 between the as-quenched state and the sample annealed at 400 °C, then it increases rapidly and eventually reaches a value four times larger in the sample annealed at 700 °C than in the one annealed at 400 °C.

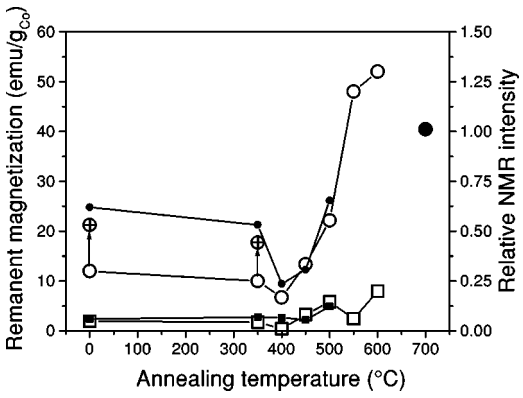

FIG. 8. A comparative superposition of the two components of remanent magnetization (open, large symbols) and the intensity of the NMR signal (closed, small symbols) in the two magnetic phases as a function of annealing temperature. The NMR intensities are scaled in such a way as to coincide with the magnetization data in the sample annealed at 700 °C (a large full circle). The two large crossed circles describe the high T_b magnetization component corrected for the change of prevailing anisotropy from uniaxial to cubic at 400 °C (see the text for details).

III. DISCUSSION

In the as-quenched sample, both NMR and remanent magnetization measurements show that cobalt is present in three distinct populations at 4.2 K one paramagnetic (or superparamagnetic) population and two ferromagnetic populations that can be separated on the basis on their different properties. These properties are: their average blocking temperature determined from magnetization measurements (about 35 and 150 K, respectively), their magnetic stiffness derived from NMR (restoring fields of about 2 and 13 kOe, respectively), and their composition determined from NMR (an alloy containing about 20 at. % of Cu and, on the other hand, pure Co particles).

The comparison between the remanent magnetization and the NMR intensity of the two magnetic phases is presented in Fig. 8 as a function of annealing temperature; it shows a clear parallel between the results of the two techniques. For the sake of comparison the NMR intensities are scaled so that they coincide with the magnetization data in the single phased sample that was annealed at 700 °C. It is clear from Fig. 8 that for all other samples there is a reasonable quantitative agreement between the two techniques.

We cannot compare the intensities of the third component, paramagnetic at 4.2 K because they are only partly probed by the two techniques. Such comparison would be even meaningless considering the different characteristic times of the measurements. E.g., the particles with a blocking temperature between 2 and 4 K for a time scale of 60 s do not contribute to the remanent magnetization at 4.2 K. On the other hand, the same particles are blocked at 4.2 K for the NMR time scale (about 20 μs the duration of the spin-echo

sequence) and, consequently, are observed by this technique.

The most visible disagreement is seen for the hard (high-T_b) phase at low annealing temperatures. This disagreement could be explained by the different shape of the pure Co clusters below and above $T_{an}=400\,^{\circ}\mathrm{C}$. Most probably the irregular clusters in the as-quenched state are dominated by a uniaxial shape anisotropy while the more spherical clusters observed in samples annealed at high temperatures show a cubic magnetocrystalline anisotropy. In such a case, for randomly oriented particles, the remanent magnetization for $T_{an}<400\,^{\circ}\mathrm{C}$ should be corrected by a factor 0.886/0.5.[26] If this correction is performed, the agreement between the two techniques becomes rather good. However, varying interactions between the particles present in samples that were annealed at different temperatures may also be responsible for the difference between the results of the two observations. Indeed, the interactions affect directly the remanent magnetization whereas their effect on the NMR intensity is corrected for, even though they do contribute to the restoring field.

Finally, let us remark that a full agreement between the two measurements is not expected anyway since the phase identification is performed on the basis of related, but not exactly similar, magnetic properties. In case of the magnetization measurements it is the full anisotropy energy KV of the particles, whereas for the NMR measurements it is the anisotropy constant K (if the particles are single domain). As already mentioned before, if both kinds of magnetic particles had about the same average volume then both techniques would probe exactly the same populations. In the present case, the ratio of the average blocking temperature for the two populations probed by the magnetic measurements is about 5:1 whereas the ratio of their average restoring field probed by NMR is about 7:1. This shows that the average volume of the particles of both kinds is actually comparable and explains the overall agreement between the two techniques.

Therefore the sample's evolution with the annealing treatment that is deduced from the present study can be summarized as follows: For annealing temperatures between 350 and 400 °C, the quenched-in Co agglomerates, mostly nonspherical and magnetically hard, are quickly dissolved and disappear. This is understood if they are located in defective regions where the atomic diffusion is enhanced. Only the largest, unstrained, and softer Co clusters are left in the sample annealed at 400 °C—as a result, the remanent magnetization reaches a minimum for this sample. Contrary to that, the alloyed (magnetically soft) component is virtually unchanged, both in terms of abundance and of composition.

When the annealing temperature is increased above 400 °C, small and strained Co clusters are nucleated again. Their interface with the matrix is much sharper than in case of the quenched-in agglomerates because their shape is more spherical and because the cobalt concentration in the alloy around them is heavily depressed. Despite their more regular shape, these new clusters are as stiff as the quenched-in ones: this observation must be related to the fact that stronger interactions between the particles set in and continuously increase up to $T_{an}=600\,^{\circ}\mathrm{C}$.[15] The volume of these clusters increases with increasing annealing temperatures as a result of a regular ripening process and the strains diminish. As the bulk diffusion increases, Co atoms that are originally present in the alloyed phase seem to undergo a different process of segregation. Between 400 and 550 °C a rapid evolution of the concentration profile takes place, the Co-rich regions get progressively richer in cobalt and, eventually, they develop a pure Co core at $T_{an}=500\,^{\circ}\mathrm{C}$.

Above $T_{an}=500\,^{\circ}\mathrm{C}$, the two kinds of particles become too similar to be distinguished by NMR. Both processes (the spinodal decomposition and Co nucleation and growth) end in formation, at $T_{an}=700\,^{\circ}\mathrm{C}$, of large, pure (or nearly pure) Co clusters that are ferromagnetic up to 400 K at least.

The present view of the inhomogeneous dispersion of cobalt in the sample is in qualitative agreement with the FIM and TEM structural investigations. Indeed the difficulty for these techniques to observe Co clusters in the as-quenched state can be explained by the shape of the latter, which is far from spherical. In the annealed samples the structural investigations, in agreement with our results, show the presence of much more spherical Co granules. Both studies also agree on the presence of a large fraction of atomically dispersed Co atoms in copper even after annealing at 450 °C. There is a striking similarity between the way the Co concentration (as seen by NMR) gets progressively larger and larger in the alloyed magnetic particles, and the spinodal-like decomposition, with a large concentration modulation, as imaged by the FIM and TEM observations.[11,12]

This large concentration modulation, along the well defined crystallographic directions, suggests an analogy with the Co/Cu multilayers. This led the authors of the above FIM/TEM study[11,12] to consider the possibility that the good GMR properties reported in the samples[27] could be assigned to the modulated structure rather than to the spherical Co clusters. However, there is no reported value of the cluster density in that study. Actually, in our sample annealed at 450 °C the pure (or nearly pure) Co clusters represent about one third of the Co content (Table II) which is confirmed by the saturation magnetization values measured in the same sample (Fig. 3 in Ref. 15). This corresponds to 3–4 % of the volume of the sample. A similar estimate was obtained by another AP/FIM study (Table I in Ref. 13). Correspondingly, the concentration modulated structure would concern two thirds of the Co content and occupy more than 95% of the sample's volume. Hence it is reasonable to raise the question about the role played by the modulated structure in the GMR effect. However, the present study shows that, within the modulated alloyed structure, the atomic fraction of cobalt that behave collectively as ferromagnetic at 4.2 K is very small: 5% of the Co content that represent a volume fraction of 0.6% in the sample (taking into account the composition of the particles). Therefore the great most of the Co-rich alloyed particles that result from the modulated concentration are not blocked down to temperatures as low as 4 K. Whether they behave as superparamagnetic particles at room temperature or merely as a collection of paramagnetic moments is clearly an open question. However, former magnetization study[15] shows that at room temperature the response of this phase to an external magnetic field up to 60 kOe is

extremely weak. Therefore there is almost no reorientation of Co magnetic moments in such field with respect to their arrangement at 0 kOe field, which would be a prerequisite for GMR. Consequently, almost no GMR associated with this compositionally modulated phase is expected, even for sample treated around 450 °C, i.e., the optimum annealing temperature for GMR.

IV. CONCLUSIONS

In conclusion, the present NMR analysis has revealed that in the studied $Co_{10}Cu_{90}$ melt spun samples Co is involved in two main structural components with distinctly different properties. The magnetically stiff component consists of small Co agglomerates—in the as-quenched sample they involve about 60% of all Co atoms. These agglomerates have irregular shapes and are located probably in heavily defected areas, such as grain boundaries. As a result of annealing around 400 °C they get quickly dissolved and the amount of Co located in those particles drops down to 24%. At the annealing temperatures of 450 °C and higher, they are replaced by more regular, spherical Co particles, which undergo a regular ripening process until they represent 100% Co at 700 °C. From the analysis of the thermoremanent magnetization this component is seen as a population with an average blocking temperature between 150 and 200 K.

The second structural component consists of CoCu alloyed particles with large concentration fluctuations. Our analysis indicates that only a small part of this population displays collective ferromagnetism at 4.2 K. This ferromagnetic part (seen in NMR as the soft magnetic phase) represents 6% of all Co atoms in the as-quenched state and its spectrum can be reproduced by a combination of two random alloys with Cu concentration of 5 and 24 %, respectively. The thermoremanence studies indicate that this phase has an average blocking temperature of about 35 K. The remaining 34% of the Co atoms in the as-quenched sample are involved in alloy particles, which are still paramagnetic or superparamagnetic at 4.2 K. Upon annealing at 450 °C and above, the concentration profile of the alloyed particles gets progressively sharper. It eventually leads to a segregation of pure Co clusters, which is seen as a new NMR line, corresponding to pure Co. At annealing temperatures larger than 500 °C Co particles formed as a result of this process do not differ from those formed by nucleation and growth.

In other words, our study reveals two parallel decomposition processes taking place in the sample as a result of annealing. One is a regular nucleation and growth of spherical Co particles and the other one resembles a spinodal decomposition of the quenched-in CoCu alloy, as already reported in Refs. 11, 12, and 14. As a result of decomposition, the amount of Co involved in the compositionally modulated alloy increases from about one-third of all Co atoms in the as quenched sample up to two-thirds in the sample annealed at 450 °C. However, in spite of the large proportion of Co involved in this phase, its contribution to GMR is expected to be rather weak, compared to that arising from the other structural component (small Co crystallites).

ACKNOWLEDGMENTS

The authors would like to thank R. Poinsot from the Institut de Physique et Chimie des Matériaux de Strasbourg, France, for taking the thermoremanence data and P. Tiberto and F. Vinai from Istituto Elettrotecnico Nazionale Galileo Ferraris, Torino, Italy, for supplying the as-quenched ribbons. This research has been supported in part by a grant from Ford Motor Company to the NMR group in the Institute of Physics, Polish Academy of Sciences. The Brazilian group has benefited from the financial support by FAPESP and CNPq.

[1] E. C. Stoner and E. P. Wohlfarth, Philos. Trans. R. Soc. London, Ser. A **240**, 599 (1948) [reprinted by IEEE Trans. Magn. **27**, 3475 (1991)].

[2] *Science and Technology of Nanostructured Magnetic Materials*, Vol. 259 of NATO Advanced Study Institute, Series B: Physics, edited by G. C. Hadjipanayis and G. A. Prinz (Plenum, New York, 1991).

[3] A. E. Berkowitz, J. R. Mitchell, M. J. Carey, A. P. Young, S. Zhang, F. E. Spada, F. T. Parker, A. Hutten, and G. Thomas, Phys. Rev. Lett. **68**, 3745 (1992).

[4] J. Q. Xiao, J. S. Jiang, and C. L. Chien, Phys. Rev. Lett. **68**, 3749 (1992).

[5] A. B. Pakhomov, X. Yan, and Y. Xu, Appl. Phys. Lett. **67**, 3497 (1995).

[6] F. C. S. da Silva, E. F. Ferrari, and M. Knobel, J. Appl. Phys. **86**, 7170 (1999).

[7] B. Idzikowski, U. K. Rossler, D. Eckert, K. Nenkov, and K. H. Muller, Europhys. Lett. **45**, 714 (1999).

[8] H. K. Lachowicz, A. Sienkiewicz, P. Gierlowski, and A. Slawska-Waniewska, J. Appl. Phys. **88**, 368 (2000).

[9] P. Allia, M. Coisson, M. Knobel, P. Tiberto, and F. Vinai, Phys. Rev. B **60**, 12 207 (1999).

[10] E. F. Ferrari, W. C. Nunes, and M. A. Novak, J. Appl. Phys. **86**, 3010 (1999).

[11] R. Busch, F. Gartner, C. Borchers, P. Haasen, and R. Bormann, Acta Mater. **43**, 3467 (1995).

[12] R. Busch, F. Gartner, C. Borchers, P. Haasen, and R. Borman, Acta Mater. **44**, 2567 (1996).

[13] W. Wang, F. Zhu, J. Weng, J. Xiao, and W. Lai, Appl. Phys. Lett. **72**, 1118 (1998).

[14] A. Lopez, F. J. Lazaro, R. von Helmholt, J. L. Garcia-Palacios, J. Wecker, and H. Cerva, J. Magn. Magn. Mater. **187**, 221 (1998).

[15] A. D. C. Viegas, J. Geshev, L. S. Dorneles, J. E. Schmidt, and M. Knobel, J. Appl. Phys. **82**, 3047 (1997).

[16] R. H. Yu, X. X. Zhang, J. Tejada, M. Knobel, P. Tiberto, and P. Allia, J. Appl. Phys. **78**, 392 (1995).

[17] M. G. M. Miranda, G. J. Bracho Rodríguez, A. B. Antunes, M. N. Baibich, E. F. Ferrari, F. C. S. da Silva, and M. Knobel, J.

Magn. Magn. Mater. **185**, 331 (1998).
[18] R. W. Chantrell, M. El-Hilo, and K. O'Grady, IEEE Trans. Magn. **27**, 3570 (1991).
[19] M. Malinowska, M. Wojcik, S. Nadolski, E. Jedryka, C. Meny, P. Panissod, M. Knobell, A. D. C. Viegas, and J. E. Schmidt, J. Magn. Magn. Mater. **198–199**, 599 (1999).
[20] S. Nadolski, M. Wójcik, E. Jedryka, and K. Nesteruk, J. Magn. Magn. Mater. **140–144**, 2187 (1995).
[21] C. Mény, E. Jedryka, and P. Panissod, J. Phys.: Condens. Matter **5**, 1547 (1993).
[22] J. P. Jay, Ph.D. thesis, Université Louis Pasteur, Strasbourg, 1995; C. Mény, Ph.D. thesis, Université Louis Pasteur, Strasbourg, 1994.
[23] H. A. M. de Gronckel, K. Kopinga, W. J. M. de Jonge, P. Panissod, J. P. Schillé, and F. J. A. den Broeder, Phys. Rev. B **44**, 9100 (1991).
[24] P. Panissod, J. P. Jay, C. Mény, M. Wójcik, and E. Jedryka, in *Magnetic Ultrathin Films, Multilayers and Surfaces*, edited by A. Fert, H. Fujimori, G. Guntherodt, B. Heinrich, W. F. Egelhoff, Jr., E. E. Marinero, and R. L. White, MRS Symposia Proceedings No. 384 (Materials Research Society, Pittsburgh, 1995), pp. 61–71.
[25] D. Kechrakos and K. N. Trohidou, Phys. Rev. B **58**, 12 169 (1998).
[26] M. Walker, P. I. Mayo, K. O'Grady, S. W. Charles, and R. W. Chantrell, J. Phys.: Condens. Matter **5**, 2779 (1993).
[27] J. Wecker, R. von Helmolt, L. Schultz, and K. Samwer, Appl. Phys. Lett. **62**, 1985 (1993).